Autofluorescence guided welding of heart tissue by laser pulse bursts at 1550 nm

KARINA LITVINOVA,[1,*] MARIA CHERNYSHEVA,[2] BERTHOLD STEGEMANN,[1] AND FRANCISCO LEYVA[1,3]

[1]*Aston Medical School, Aston University, Aston Triangle, B4 7ET, Birmingham, UK*
[2]*Leibniz Institute of Photonic Technology, Albert Einstein str 9, 07745, Jena, Germany*
[3]*Cardiology Department, Queen Elizabeth Hospital, Mindelsohn Way, B15 2TH, Birmingham, UK*
[*]*k.litvinova@aston.ac.uk*

Abstract: Wound healing and other surgical technologies traditionally solved by suturing and stapling have recently been enhanced by the application of laser tissue welding. The usage of high energy laser radiation to anastomose tissues eliminates a foreign body reaction, reduces scar formation, and allows for the creation of watertight closure. In the current work, we show that an ultrafast pulsed fibre laser beam with 183 μJ·cm^{-2} energy fluence at 1550 nm provides successful welding of dissected chicken heart walls with the tensile strength of 1.03±0.12 kg·cm^{-2} equal to that of native tissue. The welding process was monitored employing fluorescence spectroscopy that detects the biochemical composition of tissues. We believe that fluorescence spectroscopy guided laser tissue welding is a promising approach for decreasing wound healing times and the avoiding risks of postoperative complications.

1. Introduction

One of the most important tasks of modern surgery is the development of new minimally invasive methods of connecting organs and tissues. The key requirements for novel approaches enabling their implementation in clinical practice are simplicity in execution for the surgeon and leniency for the patient. The implementation of these conditions ensures the reliability of the connection of organs or tissues, guaranteeing their functioning in the early postoperative period and the fast recovery of functions of an operated organ. Still, well-developed traditional methods of restoring the integrity of the tissue, such as application of suture materials [1], metal brackets, staplers [2], adhesive compositions, are not a universal remedy. Particularly, suture materials, including nanoparticle-based glues, do not allow corrections of wound closure after application [1], while metal brackets or staplers do not form watertight closure, which can cause inflammations. Therefore, a valid alternative should be found.

Shortly after their invention, lasers have become a versatile tool in numerous medical applications [3–6], where laser surgery has been of particular interest. Laser surgery distinguishes from other traditional areas of surgery by the possibility of dissection, ablation, evaporation and welding of biological tissues with minimal concomitant injuries, reducing the likelihood of wound infection and minimising blood loss during surgery. Remarkably, laser tissue welding (LTW) provides fusing or uniting of edges of two opposing biological tissue segments by the photoexcitation of their native chromophores and water, where only light acts as the bonding catalyst [7–10]. Numerous studies using a range of histological and morphological methods confirmed that the welding of the tissue occurs by the fusion of collagen and elastin fibres [11–13]. Therefore, the LTW has been introduced as a promising and elegant solution for minimally invasive connection of organs and tissues, as it can be effectively used in both in the open and closed surgical fields, *e.g.* for the healing of internal wounds [14–16]. The LTW ensures the tightness of the wound, even in the cases of severe bleeding, without compression of the seams of tissues, avoiding marginal necrosis, and reducing the formation of a rough scar. Such wound

closures are quite challenging to do with glue and applying solders, as these could be washed off or partially diluted. Thus, in vascular and heart surgery, LTW can be used to fix patches on the vessel wall defect, with the goal of haemostasis [17,18]. In pulmonary surgery LTW enables effective closure of large wound surfaces that arose after resection of the lung or isolation of the lung from adhesions, closure small bronchial fistulas, sealing and strengthen the suture line of the anastomosis or bronchus stump [19]. LTW is advantageous for abdominal surgery, or in urology, particularly during kidney transplantation [20–22].

The first introduction of Nd:YAG laser for microvascular anastomosis of rat carotid and femoral arteries [23] was followed by the wide acceptance of laser welding technique in numerous clinical applications. Since then, various approaches and types of lasers at Near-and short-wave-IR and visible wavelength range have been suggested, including carbon dioxide, Tm:YAG, GaAlAs, argon lasers [24]. Thus, Tang et al. reported Near-IR Forsterite and Cunyite tunable lasers used for successfully welded rat skin [25]. However, these discrete and disembodied studies demonstrated low reliability and reproducibility of results of welding, and, more importantly, low strength of the repair, insufficient for practical applications. Therefore, laser welding has not been widely transferred to the clinical setting. At the same time, generally bulky design of laser systems with free space optics also could not fulfil requirements for translation into a surgery room application. This obstacle has been overcome with the introduction and rapid development of fibre laser technology, which has allowed for flexible delivery of the light onto or into a patient.

In this paper, we present a novel concept of LTW in *in vitro* chicken hearts dissection model, combined with the built-in multifunctional diagnostic optical fibre-based biosensor. We capitalised on the advantageous performance of burst mode ultrashort pulse generation [26] to achieve effective heat transfer over laser-tissue interaction. We show promising capabilities of 1550 nm-ultrafast fibre laser generating bunches of femtosecond pulses to anastomose dissected heart tissues. The choice of the laser is explained by several factors, the main among which is the high water absorption compared to Near-IR spectral range. Also, the availability of all-fibre components, due to application in telecommunications, makes ultrafast Er-doped fibre lasers compact, robust and cost-efficient systems. It has been noted that when welding with pulsed lasers at 1550 nm, the water in the collagen helix absorbs the pulse energy and immediately hikes to a significantly higher temperature than the surrounding tissue [27]. Here, a high intraburst pulse repetition rate of 25 GHz enables higher heat diffusion in the tissue. At the same time, a longer time delay of 41 ns-time between the bursts allows cooling of material and prevents its degradation [26]. To avoid the risk of over-treating the target location and minimising tissue damage [28], the LTW has to be continuously monitored by fluorescence spectroscopy, which allowed observation of changes in the biological tissue area exposed to laser irradiation. *Alfano* and his group employed non-invasive fluorescence and Raman spectroscopy to measure the effects of welding on biochemical composition of tissues and changes in collagen and elastin before and after LTW [29,30]. The developed technology displayed good repetitiveness of the welding results with near-native tissue's tensile strength of 0.1 Mpa. Hand-held laser delivery fibre, without application of a computer-controlled sample positioning stage [31], mimics a realistic scenario in the surgery room. We believe that the current study presents an encouraging starting point for more sophisticated investigation *in vivo* tissue or aorta welding processes.

2. Methods and materials

The schematic of the LTW system, presented in Fig. 1(a), consists of an ultrafast laser, hand-held laser delivery fibre with lenses for efficient light focusing. The welding process is controlled by fluorescent spectroscopy, which signal is collected via fibre probe and *in situ* analysed via PC.
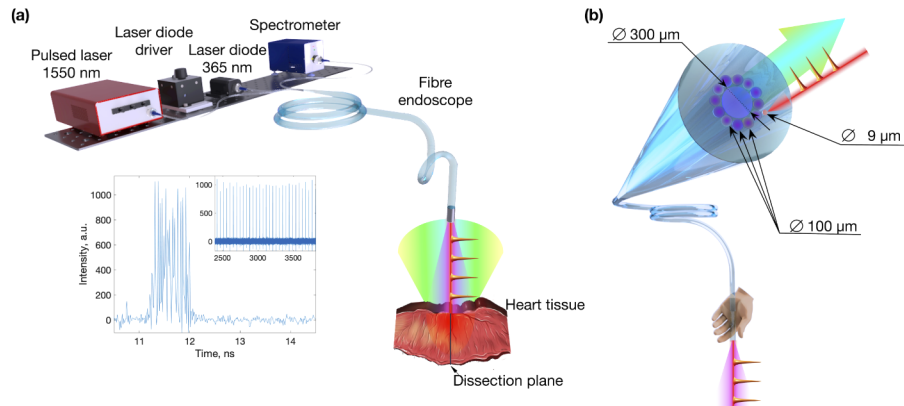
Fig. 1. Laser tissue welding assisted by fluorescence spectroscopy. a) Experimental setup. Inset: Pulse train of ultrafast laser. b) Schematic of multifunctional fibre probe.

2.1. Laser system design

To perform welding of myocardium tissue, a customised ultrafast fibre laser, operating at 1550 nm, has been developed similar to the one published in [32], followed by Er-doped fibre amplifier. The main feature of the laser performance is the operation in the burst mode [26]. Pulse bursts present short successions of ultrashort pulses at high repetition rate (in the GHz order). Bursts in their turn repeat at a lower rate, which corresponds to the fundamental frequency of the fibre laser – in the MHz order. Figure 1(a) shows characteristic pulse burst trace. Contrary to the laser system, presented in Ref. [26], where the bursts of pulses were formed by multiplying the repetition rate of seed laser followed by cropping the bursts, in the current laser system the burst were formed due to soliton energy quantisation and balanced attraction between pulses. Thus, the reduction of the cost-metric parameter of the laser system comes at a price of uniform intraburst intensity.

Such duty cycle is beneficial for tissue interaction, as it allows decreasing the energy of individual pulses with the increase of the generated average laser power, dividing it by a number of pulses in the burst. Due to their ultrashort duration, femtosecond pulses do not cause shock waves and heat conduction into the surrounding tissue and, therefore, produce no collateral damage in the laser-irradiated material [33]. Since the heating of tissues is proportional to the pulse repetition rate, the sequence of pulses insight the burst lowers the welding threshold allowing to accumulate their energy. Therefore, the burst mode generation is an efficient approach to enable effective welding by using significantly lower laser powers, compared to previously reported works [34,35].

In the experiment, the laser system operated with an average power of 580 mW at a burst repetition rate of 21.5 MHz. The burst consists of 20 pulses with a duration of 380 fs and intraburst pulse repetition rate of ~25 GHz, corresponding to pulse separation of 40 ps (Fig. 1(b)). Assuming the uniformity of pulse intensities, the energy of the individual pulse is ~1.35 nJ. Even though the inset in Fig. 1 demonstrates that pulses did not have equal intensities within bursts, particularly at its edges, this feature did not obstruct the intended application for tissue welding. The laser light generation was delivered through the single-mode optical fibre with a core diameter of ~9 μm within the endoscope probe (see Fig. 1(b)), producing a light spot on the tissue of about 2 mm in diameter with the resulting launched pulse intensity of ~1.7 mW·cm^{-2}. The distance between tissue and laser catheter was approximately 1 cm, which allowed good observation of the welding process and secure placement of probe for fluorescent spectroscopy.

2.2.　Sample preparation and tensile strength assessment

A total number of 25 chicken hearts from H Bellingham Ltd (Birmingham Wholesale Market, UK) were studied. In preparation of the study, sections of 6 mm in thickness were dissected into halves with the area of around 2 cm^2. Samples were transported, and maintained in small, covered Petri dishes with saline solution, which prevented their drying and deterioration of tissue. Petri dishes were placed on a bed of ice at all times. Twenty-five samples were welded and sent for histopathological evaluation. Snap-frozen samples were cut into thin sections using a cryostat and stained for Hematoxylin and Eosin (H&E). H&E stained welded tissues were imaged using the NanoZoomer digital slide scanner (Hamamatsu). Another set of 25-welded samples were subjected to a tensile test to check the strength of the resulting weld.

Due to unavailability of calibrated strength gauges, the tensile strength measurements were performed using the improvised tensometer (see Fig. 2(c)), similar to presented in [36]. The welded tissue was suspended in a clamp. The other clamp was attached to the lower part of welded tissue along with the small weights. Tiny loads were gradually added until a gap originated in the weld. The weight of the end clamp (6 g) was added to the weight of the total amount of the weights and then fixed as the breaking load.
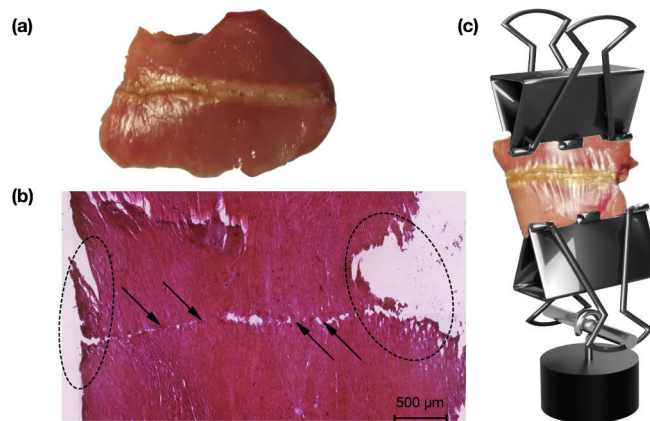

Fig. 2. Results of laser tissue welding using ultrafast laser at 1550 nm. a) Welded heart sample. b) H&E stained welded heart sample. Black arrows indicate the closure line. Circles show increased intensity of H&E stain indicating minor thermal damage at both edges. c) Schematic of stretch test.

2.3.　Autofluorescence monitoring

The fluorescence spectroscopy was used before, during and after LTW to analyse the thermal effects on biochemical composition of tissues and measure changes in collagen, elastin, NADH and flavins [37]. We used the prototype of the biosensor with fibre coupled LED, operating at a fluorescence excitation wavelength of 365 nm. Resultant tissue fluorescence emission was recorded across a wavelength range from 380 to 800 nm using a spectrometer and processed using custom-made software (SPE LAZMA Ltd., Russia) [38]. Fluorescence measurements were performed through custom made fibre probe 1.6 mm in diameter, consisting of 12 multi-mode optical fibres with a core diameter of 100 μm for delivering light from LEDs, and fluorescence signal collecting fibre with a core diameter of 300 μm (Fig. 1(b)). The numerical aperture of the fibres was 0.22. Fluorescence analysis of fluorophores at different excitation wavelengths was performed and presented as the coefficient of fluorescent contrasts [39]. We check the assumption of normality distribution using the Shapiro-Wilk test using a *p* value of 0.01. For normal distributed rate, the comparisons were conducted using a parametric unpaired t-test.

3. Results

The selection of laser power was performed by monitoring of autofluorescence of the exposed heart samples. The critical feature manifesting the beginning of welding process was the growth of the fluorescence peak at around 420-455 nm, corresponding to elastin and collagen, and appearance of the peak at 570 nm, characteristic for metHb [40] (see Fig. 3, Table 1).
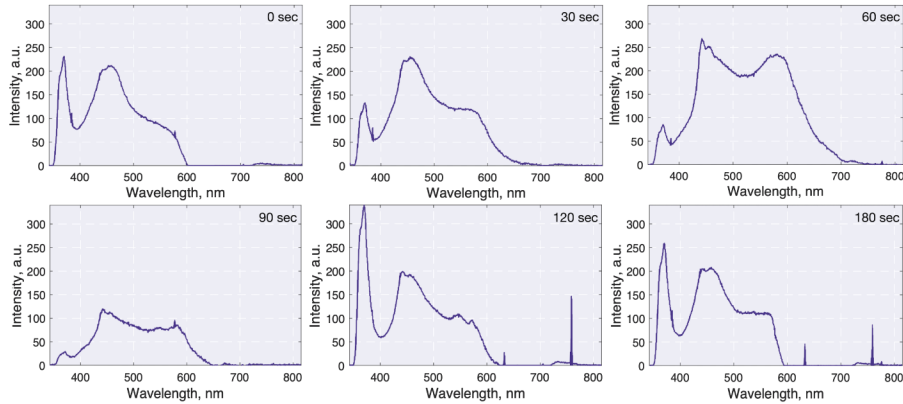

Fig. 3. 365 nm fluorescence real-time monitoring of the welding procedure. Time is stated from the beginning of welding.

Table 1. Displays the averages of measured fluorescence coefficient values for each of the measured heart samples during welding.

Type of fluorophore	Registered wavelength, nm	Coefficient of fluorescent contrasts at welding exposure time			
		0 sec	30 sec	60 sec	180 sec
Collagen	420	0.35±0.11	0.60±0.14	0.80±0.10[a]	0.25±0.90[b],[c]
Elastin	450	0.50±0.10	1.01±0.14	0.93±0.08[a]	0.43±0.11[b],[c]
NADH	490	0.71±0.70	0.81±0.04	1.11±0.06[a]	0.12±0.02[a],[b],[c]
FAD	550	0.28±0.06	1.08±0.24	0.82±0.10[a]	0.07±0.05[a],[b],[c]
Haemoglobin/myoglobin	580-590	0.29±0.04	0.69±0.06	0.91±0.04[a]	0[a],[b],[c]

[a]Statistically significant difference with the start point, ($p < 0.05$)
[b]Statistically significant difference with the 30 sec point, ($p < 0.05$)
[c]Statistically significant difference with the 60 sec point, ($p < 0.05$)

Preliminary studies of various laser operation regimes and output parameters have demonstrated that optimal average laser power to achieve reliable and repeatable heart tissue welding was ~580 mW. At a burst repetition rate of 21.5 MHz and intraburst pulse spacing of 40 ps, relatively low launched pulse intensity (of ~1.7 W·cm^{-2}) allowed to eliminate the risk of non-linear tissue interactions and potential ablation and tissue carbonisation. The hand-held laser probe was moved along the apposition line always in one direction. This produced consecutive one-second laser radiation exposures per 1.4 cm length of anastomosis (around 1 sec per beam spot diameter) followed by approximately 9 seconds of cooling. Such low time of tissue exposure to laser irradiation compared to cooling also allows avoiding the risk of irreversible thermal damage. Overall, 20 round trips were made with the probe along the closure, resulting in 180-sec exposure. Our light absorption and heat conduction simulations showed that most tissue heating occurred within 2 mm from the surface. With an average incident power of 580 mW, an absorptive core of 2 mm diameter, an absorption coefficient of 10 cm^{-1} and passive heat conduction of cardiac tissue

the simulations demonstrate the repetitive heating and schooling scheme led to a well-controlled increase in temperature within the target temperature range of 50-60° C.

All dissected hearts samples were successfully welded (Fig. 2(a)). Thermal damage was restricted to the top layers only. However, as a characteristic feature of a hand-held LTW probe moving along the closure line, edges of the wound received substantially higher exposure to laser irradiation. Figure 2(b) shows a few areas of vacuolisation and carbonisation at the margins of closure line (circled areas). Apart from those, no signs of thermal tissue damage associated with the LTW process was observed.

We were able to qualitatively assess laser-welded tissue using fluorescence spectroscopy, which enables monitoring of changes in key protein and lipid molecules in real-time during the LTW process (Fig. 3). Coefficients of fluorescent contrasts of fluorophores at after 0, 30, 60 and 180 sec from the beginning of the welding are summarised in Table 1. Presented average values are means ±SEM.

The tensile strength measurements (see Fig. 2(c)) demonstrated strengths of welded chicken heart tissue equal to that of native tissue (0.11 Mpa [36], based on statistical testing. The mean tensile strength for 25 samples 1.03 ± 0.12 kg·cm^{-2} (10.09 ± 1.17 N·cm^{-2} or 0.1 Mpa). The weld could endure a weight force density of 20 W·cm^{-2} at 6° load angle.

4. Discussion

LTW is an experimental technique designed as an alternative to sutures. The standard stitches are favoured because they are cost-effective, reliable, and suitable for almost any type of tissue. However, due to their mechanical invasion, the use of the sutures, staples, and clips causes tissue injury. In comparison to conventional suturing, LTW is the potentially less traumatic, faster and easier procedure for minimally invasive surgery, providing immediate watertight sealant.

Generally, ultrashort laser pulses are applied for effective surface ablation and evaporation of material. However, in our experiment, the proper selection of wavelength and laser operation mode allowed the achievement of different light-tissue interaction, affecting 6 mm in the depth of heart tissues. Light at 1550 nm is effectively absorbed in biological tissue. As shown in Fig. 4 the energy transport inside the tissue sample exposed to laser radiation at 1550 nm is determined by passive heat conduction due to higher absorption coefficient, mainly of water. Such strong light-tissue interaction is exceptional to 1550 nm wavelength. In comparison, the absorption and temperature distribution in the sample under 980-nm radiation shows much smaller effects [41]. Similarly, in Ref. [42] it was demonstrated that LTW using adjacent radiation wavelength of 1430 nm was more effective than that using 1250 nm. With a longer time of laser radiation exposure, heat conduction starts playing a more significant role than the distribution of the optical power density. Thus, here a large portion of ultrashort pulses energy contributes not to the ablation of the surface of the sample but conducted to lower tissue layers.

Earlier published works studied how collagen and elastin can be cross-linked by thermal effect. The theory is that protein bonds located near the anastomotic line are degraded thermally; allowing proteins to rebind to adjacent proteins and cause new molecular bonds which are stabilised by cooling and produce welding effect [24,43,44]. The effective temperature for LTW depends on wavelength, type of tissue and laser parameters. The literature review shows that required temperatures for laser tissue welding, with collagen and elastin as the major bonding components, are in the range of 60 to 80° C [45,46]. At the same time, the determination of more accurate temperatures is difficult because thermal coagulation of binding proteins is a rate process driven by energy, rather than the temperature threshold [47].

To understand better tissue temperature increase induced by laser irradiation, it was simulated using Comsol (Comsol 4.3). In the model, we used a circular tissue structure of 10 cm in diameter and 6 mm in thickness. We assumed that the tissue is clamped to a heat sink, which temperature at the radial border and the bottom disc was fixed at 20° C. The other sides were
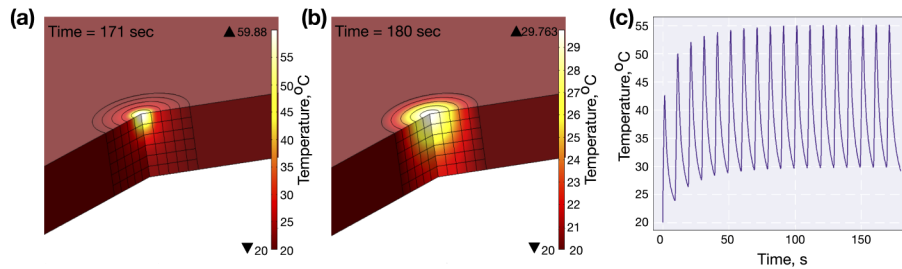
Fig. 4. The experimental protocol with a duty cycle of one second heating and nine seconds cooling caused a well controllable and gradual heating of the tissue demonstrated by our numerical simulation. (a,b) simulated three-dimensional temperature distribution in heart sample at 171 ans 180 sec from the beginning of welding, (c) simulated transients of mean temperature of the 1 mm layer underneath the heated surface

thermally isolated. We used heat capacity and conductivity of passive myocardial tissue [48]. No perfusion induced cooling was taken into consideration. We assumed that the incident laser light was absorbed by tissue volume within the cylinder with a 1 mm radius and 6 mm thickness, serving as the heat source. The radius of the cylinder matched the beam size. The beam was directed orthogonally at 2 mm spot on the tissue.

Light absorptive heat generation at 1550 nm was modelled using Monte Carlo simulation, taking up biological tissue absorption μ_a and scattering μ_s coefficients of 10 cm^{-1} 20 cm^{-1}, correspondingly, and anisotropy of scattering, g, equal to 0.95 [49,50]. The 3D Monte-Carlo simulation data of the light distribution was projected to a 2D (planar) structure and imported into COMSOL for performing the heat diffusion analysis. The COMSOL algorithm models the diffusion problem as rotational symmetric with respect to the beam axis. Tissue heating due to ultrafast laser irradiation with an average power of 580 mW was modelled every 0.5 seconds for up to 180 seconds. Tissue heating modelling followed the experimental protocol. Repeated episodes of one second heating with subsequent 9 seconds of cooling were simulated.

While the sequence of ultrashort pulses within the bursts produces the saw-back pattern to the tissue temperature increase on the sub-ns time scale, similar to presented in Ref. [26]. Nevertheless, such fine structure becomes hidden in larger cooling-heating cycles related to the fibre probe movement along the line of tissue closure. Our model considers only larger cycles, where the temperature increase has a linear trend. The results of the numerical model of the ultrafast fibre laser heat transfer are shown in Fig. 4. Figures 4(a,b) demonstrate simulated temperature distribution in the tissue at the end of heating and cooling periods respectively. More than 95% of light energy was absorbed within the light absorptive cylinder of 6 mm length, as shown in Fig. 4(a). While between the periods of laser irradiation, the heat is conducted to surrounding tissues, which results in the wider radial distribution of the tissue temperature (Fig. 4(b)). Figure 4(c) confirms that the selected laser generation regime and welding mode allowed us to control the level of the mean temperature of the 1-mm layer underneath the irradiated surface in the range from 50 to 60° C. As temperature (laser energy) rises and heating times are prolonged, cellular and tissue structural proteins undergo denaturation and conformational changes. Heat-denatured collagen unwinds its helix structure to expose sections for intermolecular interactions. However, collagen superhelix is mostly stabilised by cooperative interactions from a large number of weak, reinforcing bonds. It was hypothesised, that if one bond is lost, adjacent bonds are quickly broken, resulting in adhesion instability [51,52].

At the present study, the control of laser power and duration of laser irradiation was performed by autofluorescence monitoring of exposed cardio tissues. During the welding process, we maintained a high level of fluorescence of collagen/elastin, suggesting that such a regime will

be beneficial for the structural proteins to bind together. Histological analysis confirmed our assumption: no severe damage to the cells along the welded cut was observed. The fluorescence spectroscopy presented a valuable objective endpoint determination of the welding process, which played an important role in the high degree of reproducibility of the welding, similar to [53]. We attribute the occurrence of minor damage of small areas at the beginning and end of the weld to the fact that the laser beam was delayed a little bit longer in these places while reversing welding direction. The numerical model is also in good agreement with the recurrent movement of the welding fibre probe demonstrating heating-cooling cycles and their effect of the weld (Fig. 4). It also worth to note that after 80th second of the welding process, the maximum temperature of mass saturated, i.e. further cycles did not increase it above the maximum of 62.7° C (Fig. 4(b)). It also confirms that the small variation of the obtained welding results during the experiments are likely caused by the learning curve of the laser operator (in a future surgeon) of using the hand-held probe with laser radiation delivery optical fibre. The welding results improved in the course of the study.

5. Conclusion

In conclusion, we have presented a technology platform for reliable biological tissue welding, based on ultrafast laser irradiation guided by fluorescence spectroscopy. The dissected chicken hearts were successfully welded without any glue or solder, showing high repeatability of the result. The tensile strength assessment confirmed the reliability of welded dissected heart samples. We have proposed a novel approach to perform simultaneous delivery of welding pulsed laser generation and diagnostic light through the multi-functional optical fibre probe. Additionally, this work shows that autofluorescence spectroscopy can give comprehensive quantitative information on changes in the tissue during welding and, therefore, *in situ* control of tissue heating according to structural proteins denaturation. Beyond the performed study, our vision is to expand this approach to other biological tissues and use for *in vivo* tissue welding, in future. The long-term study of the LTW, performed using animal models, is anticipated to evaluate wound healing dynamics.

Acknowledgments

Disclosures

The authors declare no conflicts of interest.

References

1. S. Rose, A. Prevoteau, P. Elzière, D. Hourdet, A. Marcellan, and L. Leibler, "Nanoparticle solutions as adhesives for gels and biological tissues," Nature **505**(7483), 382–385 (2014).
2. F. E. Shelton IV, J. S. Swayze, K. R. Doll, and E. L. Timperman, "Surgical stapling apparatus comprising a usage lockout," (2015). US Patent App. 14/538,446.
3. S. L. Trokel, R. Srinivasan, and B. Braren, "Excimer laser surgery of the cornea," Am. J. Ophthalmol. **96**(6), 710–715 (1983).
4. I. Pence and A. Mahadevan-Jansen, "Clinical instrumentation and applications of raman spectroscopy," Chem. Soc. Rev. **45**(7), 1958–1979 (2016).
5. A. I. Metelitsa and T. S. Alster, "Fractionated laser skin resurfacing treatment complications: a review," Dermatol. Surg. **36**(3), 299–306 (2010).
6. R. J. Min, N. Khilnani, and S. E. Zimmet, "Endovenous laser treatment of saphenous vein reflux: long-term results," J. Vasc. Interv. Radiol. **14**(8), 991–996 (2003).
7. L. S. Bass and M. R. Treat, "Laser tissue welding: A comprehensive review of current and future," Lasers Surg. Med. **17**(4), 315–349 (1995).

8. P. Matteini, F. Rossi, F. Ratto, and R. Pini, "Laser welding of biological tissue: mechanisms, applications and perspectives," *Laser Imaging and Manipulation in Cell Biology* pp. 203–231 (2010).

9. C. Li, K. Wang, and J. Huang, "Simulation of the effect of spot size on temperature field and weld forming in laser tissue welding," Optik **155**, 315–323 (2018).

10. C. Fornaini, E. Merigo, F. Poli, J.-P. Rocca, S. Selleri, G. Lagori, and A. Cucinotta, "Hard dental tissues laser welding: a new help for fractured teeth? a preliminary ex vivo study," Laser Ther. **27**(2), 105–110 (2018).

11. T. Menovsky, J. F. Beek, and M. J. van Gemert, "Laser tissue welding of dura mater and peripheral nerves: a scanning electron microscopy study," Lasers Surg. Med. **19**(2), 152–158 (1996).

12. J. Tang, D. O'Callaghan, S. Rouy, and G. Godlewski, "Quantitative changes in collagen levels following 830-nm diode laser welding," Lasers Surg. Med. **22**(4), 207–211 (1998).

13. R. A. White, G. Kopchok, S.-K. Peng, R. Fujitani, G. White, S. Klein, and J. Uitto, "Laser vascular welding—how does it work?" Ann. Vasc. Surg. **1**, 461–464 (1987).

14. Z. Nagy, A. Takacs, T. Filkorn, and M. Sarayba, "Initial clinical evaluation of an intraocular femtosecond laser in cataract surgery," J. Refract. Surg. **25**(12), 1053–1060 (2009).

15. J. P. Rodrigo, C. Suárez, C. E. Silver, A. Rinaldo, P. Ambrosch, J. J. Fagan, E. M. Genden, and A. Ferlito, "Transoral laser surgery for supraglottic cancer," Head & Neck: Journal for the Sciences and Specialties of the Head and Neck **30**(5), 658–666 (2008).

16. M.-V. Senat, J. Deprest, M. Boulvain, A. Paupe, N. Winer, and Y. Ville, "Endoscopic laser surgery versus serial amnioreduction for severe twin-to-twin transfusion syndrome," N. Engl. J. Med. **351**(2), 136–144 (2004).

17. T. K. Gayen, A. Katz, H. E. Savage, S. A. McCormick, M. Al-Rubaiee, Y. Budansky, J. Lee, and R. Alfano, "Aorta and skin tissues welded by near-infrared cr4+: Yag laser," J. Clin. Laser Medicine & Surg. **21**(5), 259–269 (2003).

18. R. B. Stewart, A. Benbrahim, G. M. LaMuraglia, M. Rosenberg, G. J. L'Italien, W. M. Abbott, and R. T. Kung, "Laser assisted vascular welding with real time temperature control," Lasers Surg. Med. **19**(1), 9–16 (1996).

19. B. S. Bleier, N. M. Cohen, J. D. Bloom, J. N. Palmer, and N. A. Cohen, "Laser tissue welding in lung and tracheobronchial repair: an animal model," Chest **138**(2), 345–349 (2010).

20. B. Lobel, O. Eyal, N. Kariv, and A. Katzir, "Temperature controlled co2 laser welding of soft tissues: Urinary bladder welding in different animal models (rats, rabbits, and cats)," Lasers Surg. Med. **26**(1), 4–12 (2000).

21. C. Bertrand and A. Poulon-Quintin, "Proposals for optimization of laser welding in prosthetic dentistry," J. Prosthodontics **19**(1), 69–76 (2010).

22. K. Ogan, L. Jacomides, H. Saboorian, K. Koeneman, Y. Li, C. Napper, J. Hoopman, M. S. Pearle, and J. A. Cadeddu, "Sutureless laparoscopic heminephrectomy using laser tissue soldering," J. Endourol. **17**(5), 295–300 (2003).

23. K. K. Jain, "Sutureless microvascular anastomosis using a neodymium-yag laser," Microsurgery **1**(6), 436–439 (1980).

24. R. Pini, F. Rossi, P. Matteini, and F. Ratto, "Laser tissue welding in minimally invasive surgery and microsurgery," in *Biophotonics*, (Springer, 2008), pp. 275–299.

25. J. Tang, J. M. Evans, V. Petricevic, P.-P. Ho, and R. R. Alfano, "Tissue welding using near-infrared forsterite and cunyite tunable lasers," IEEE J. Sel. Top. Quantum Electron. **5**(4), 1103–1106 (1999).

26. C. Kerse, H. Kalaycıoğlu, P. Elahi, B. Çetin, D. K. Kesim, Ö. Akçaalan, S. Yavaş, M. D. Aşık, B. Öktem, H. Hoogland, R. Holzwarth, and F. O. Ilday, "Ablation-cooled material removal with ultrafast bursts of pulses," Nature **537**(7618), 84–88 (2016).

27. V. Sriramoju and R. R. Alfano, "In vivo studies of ultrafast near-infrared laser tissue bonding and wound healing," J. Biomed. Opt. **20**(10), 108001 (2015).

28. A. Alimova, R. Chakraverty, R. Muthukattil, S. Elder, A. Katz, V. Sriramoju, S. Lipper, and R. Alfano, "In vivo molecular evaluation of guinea pig skin incisions healing after surgical suture and laser tissue welding using raman spectroscopy," J. Photochem. Photobiol., B **96**(3), 178–183 (2009).

29. J. Tang, F. Zeng, H. Savage, P. P. Ho, and R. Alfano, "Fluorescence spectroscopic imaging to detect changes in collagen and elastin following laser tissue welding," J. clinical laser medicine & surgery **18**(1), 3–8 (2000).

30. V. Sriramoju and R. R. Alfano, "Laser tissue welding analyzed using fluorescence, stokes shift spectroscopy, and huang-rhys parameter," J. Biophotonics **5**(2), 185–193 (2012).

31. C. Liu, W. Wang, A. Alimova, V. Sriramoju, V. Kartazayev, and R. Alfano, "Monitoring changes of proteins and lipids in laser welded aorta tissue using raman spectroscopy and basis biochemical component analyses," in *Optical Interactions with Tissue and Cells XX*, vol. 7175 (International Society for Optics and Photonics, 2009), p. 717504.

32. M. Chernysheva, M. Al Araimi, G. A. Rance, N. J. Weston, B. Shi, S. Saied, J. L. Sullivan, N. Marsh, and A. Rozhin, "Revealing the nature of morphological changes in carbon nanotube-polymer saturable absorber under high-power laser irradiation," Sci. Rep. **8**(1), 7491–7499 (2018).

33. A. Vogel, J. Noack, G. Hüttman, and G. Paltauf, "Mechanisms of femtosecond laser nanosurgery of cells and tissues," Appl. Phys. B **81**(8), 1015–1047 (2005).

34. A. I. Uba, H. O. Tabakoglu, U. A. Abdullahi, and M. M. Sani, "Closure of skin incision by dual wavelength (980 and 1064 nm) laser application," J. Cosmet. Laser Ther. **19**(2), 109–113 (2017).

35. B. Ott, B. J. Züger, D. Erni, A. Banic, T. Schaffner, H. P. Weber, and M. Frenz, "Comparative in vitro study of tissue welding using a 808 nm diode laser and a ho: Yag laser," Lasers Med. Sci. **16**(4), 260–266 (2001).

36. M.-B. Edwards, E. R. Draper, J. W. Hand, K. M. Taylor, and I. R. Young, "Mechanical testing of human cardiac tissue: some implications for mri safety," J. Cardiovasc. Magn. Reson. **7**(5), 835–840 (2005).

37. A. C. Croce and G. Bottiroli, "Autofluorescence spectroscopy for monitoring metabolism in animal cells and tissues," in *Histochemistry of Single Molecules*, (Springer, 2017), pp. 15–43.

38. O. Smirnova, D. Rogatkin, and K. Litvinova, "Collagen as in vivo quantitative fluorescent biomarkers of abnormal tissue changes," J. Innovative Opt. Health Sci. **05**(02), 1250010 (2012).

39. A. V. Dunaev, V. V. Dremin, E. A. Zherebtsov, I. E. Rafailov, K. S. Litvinova, S. G. Palmer, N. A. Stewart, S. G. Sokolovski, and E. U. Rafailov, "Individual variability analysis of fluorescence parameters measured in skin with different levels of nutritive blood flow," Med. Eng. & Phys. **37**(6), 574–583 (2015).

40. P. Lanka, F. K. Joseph, H. Kruit, S. K. V. Sekar, A. Farina, R. Cubeddu, S. Manohar, and A. Pifferi, "Time domain diffuse optical spectroscopy for the monitoring of thermal treatment in biological tissue," in *Optical Tomography and Spectroscopy*, (Optical Society of America, 2020), pp. SM2D–4.

41. M. Wehner, P. Betz, and M. Aden, "Influence of laser wavelength and beam profile on the coagulation depth in a soft tissue phantom model," Lasers Med. Sci. **34**(2), 335–341 (2019).

42. J. Tang, F. Zeng, J. M. Evans, B. Xu, H. Savage, P. P. Ho, and R. Alfano, "A comparison of cunyite and fosterite nir tunable laser tissue welding using native collagen fluorescence imaging," J. Clin. Laser Medicine & Surg. **18**(3), 117–123 (2000).

43. L. W. Murray, L. Su, G. E. Kopchok, and R. A. White, "Crosslinking of extracellular matrix proteins: a preliminary report on a possible mechanism of argon laser welding," Lasers Surg. Med. **9**(5), 490–496 (1989).

44. I. F. Cilesiz, "Controlled temperature photothermal tissue welding," J. Biomed. Opt. **4**(3), 327 (1999).

45. P. N. Prasad, *Introduction to Biophotonics* (John Wiley & Sons, 2004).

46. K. S. Marchitto and S. T. Flock, "Method and device for anastomoses," (2009). US Patent 7,588,565.

47. A. McKenzie, "Physics of thermal processes in laser-tissue interaction," Phys. Med. Biol. **35**(9), 1175–1210 (1990).

48. I. Foundation, *Heat Capacity*, https://itis.swiss/virtual-population/tissue-properties/database/heat-capacity/ (accessed: 01.06.2020).

49. S. A. Filatova, I. A. Shcherbakov, and V. B. Tsvetkov, "Optical properties of animal tissues in the wavelength range from 350 to 2600 nm," J. Biomed. Opt. **22**(3), 035009 (2017).

50. S. L. Jacques, "Optical properties of biological tissues: a review," Phys. Med. Biol. **58**(11), R37–R61 (2013).

51. W. Traub and K. A. Piez, "The chemistry and structure of collagen," in *Advances in protein chemistry*, vol. 25 (Elsevier, 1971), pp. 243–352.

52. J. Berg, J. Tymoczko, and L. Stryer, "Protein composition and structure. biochemistry," (2012).

53. J. Dong, H. Breitenborn, R. Piccoli, L. V. Besteiro, P. You, D. Caraffini, Z. M. Wang, A. O. Govorov, R. Naccache, F. Vetrone, L. Razzari, and R. Morandotti, "Terahertz three-dimensional monitoring of nanoparticle-assisted laser tissue soldering," Biomed. Opt. Express **11**(4), 2254–2267 (2020).